A Transfer Nuclear Overhauser Effect Study of Coenzyme Binding to Distinct Sites in Binary and Ternary Complexes in Glutamate Dehydrogenase†

Anirban Banerjee,‡,§ H. Richard Levy,‖ George C. Levy,‡ Charles LiMuti,⊥ Barry M. Goldstein,# and J. Ellis Bell*,⊥

Departments of Chemistry and Biology, Syracuse University, Syracuse, New York 13244, and Departments of Biophysics and Biochemistry, University of Rochester, Rochester, New York 14642

Received March 20, 1987; Revised Manuscript Received July 16, 1987

ABSTRACT: The oxidized coenzyme NAD binds to two sites per subunit of bovine liver glutamate dehydrogenase with equal affinity in the absence of dicarboxylic acid coligands. In the presence of glutarate or 2-oxoglutarate, the affinity to one site is unchanged, but the affinity to the other (presumed to be the active site) is considerably increased and now requires two dissociation constants to describe its saturation. A combination of transfer nuclear Overhauser effects (TRNOE) together with an examination of the slopes of TRNOE time dependence indicates that while NAD is bound in a syn conformation at both binding sites, NADP (which binds only to the active site) is bound in a syn–anti mixture. The existence of N6 to N3′ and N6 and N2′ and N1′ to N3′ NOE's with NAD suggests that the two coenzyme binding sites are located near enough to allow intermolecular NOE's. In the presence of 2-oxoglutarate where only binding to the active site is effectively observed, the conformation of either coenzyme is syn. Modeling studies using the distance estimates from the TRNOE results suggest that the nicotinamide ribose approximates a 3′-endo conformation. The absence of evidence for intermolecular NOE's under these conditions indicates that while the active and regulatory NAD sites per subunit are in close proximity, the six active sites per hexamer are located greater than 5 Å apart.

The L-glutamate dehydrogenase (EC 1.4.1.3) from bovine liver is typical of mammalian glutamate dehydrogenase in that it can utilize NAD(H) and NAD(P)H with near equal facility (Engel & Dalziel, 1969). The enzyme is a hexamer of chemically identical subunits (Appella & Tomkins, 1966), which have been sequenced (Smith et al., 1975). Although the hexamer undergoes a concentration-dependent polymerization (Mire & Cohen, 1971) that is affected by various ligands, it has been possible to obtain a fully active enzyme that does not undergo hexamer polymerization after chemical modification and cross-linking with dimethylpimilimidate (Smith & Bell, 1985).

Bovine liver glutamate dehydrogenase is subject to regulation by a wide variety of ligands and has been demonstrated to show negative homotropic interactions between subunits within the hexamer (Bell & Dalziel, 1973; Alex & Bell, 1980). Each subunit has two sites capable of binding NADH: the active site and a second regulatory site (Jallon & Iwatsubo, 1971). The active site binds NADH and NADPH with equal facility (George & Bell, 1980), but the regulatory site has a much lower affinity for NADPH than for NADH. The presence of a cosubstrate such as glutamate considerably enhances the affinity of NAD(P)H at the active site but appears to have no effect on the affinity of the regulatory site.

The oxidized coenzymes NAD and NADP bind much more weakly than the reduced coenzymes in the absence of a cosubstrate, and while there appear to be two NAD binding sites (Bayley & O'Neill, 1980; Smith & Bell, 1982) in the presence of the glutamate analogue glutarate, the number of sites in the binary enzyme–NAD complex remains unclear (Egan & Dalziel, 1972).

Glutamate dehydrogenase is a B-stereospecific enzyme, transferring the *pro-s* hydrogen of NAD(P)H to substrate during the reductive amination reaction (Levy & Vennesland, 1957; You, 1982). Preliminary transfer nuclear Overhauser effect (TRNOE) experiments (Levy et al., 1983) indicated that, as expected, the adenine ring was in the anti conformation and a nicotinamide ring was syn for bound coenzyme. However, these preliminary studies with the rat liver glutamate dehydrogenase also indicated conformational differences between bound NAD and NADP and suggested that, especially with NADP, a fraction of the coenzyme was bound in the "wrong" anti conformation.

In the present study we have examined in detail the conformations of the nicotinamide ring of NAD and NADP in both binary and ternary complexes. In conjunction with further binding studies of NAD to the enzyme, it is apparent that while NAD and NADP are bound to the active site in ternary complexes in a strict syn conformation, NADP in binary complexes does show a syn–anti mix. The binding of NAD in binary complexes appears to be in a syn conformation at both the active and regulatory sites. Intermolecular TRNOE's suggest that the two coenzyme binding sites must be in close proximity on the subunit.

Materials and Methods

The enzyme used in this study is bovine liver glutamate dehydrogenase, obtained from Sigma Chemical Co., that is chemically cross-linked and modified with dimethylpimil-

† This work was supported by NIH Grants GM 30195 and PHS-2507-RROS 403-24 (J.E.B.), NIH Grant RR 01317 (G.C.L.), and NSF Grant PCM 8309379 (H.R.L.).

* Address correspondence to this author at the Department of Biochemistry, University of Rochester Medical Center, Rochester, NY 14642.

‡ Department of Chemistry, Syracuse University.

§ Present address: University of Colorado Health Sciences Center, Denver, CO 80262.

‖ Department of Biology, Syracuse University.

⊥ Department of Biochemistry, University of Rochester.

Department of Biophysics, University of Rochester.

0006-2960/87/0426-8443$01.50/0

imidate as described previously (Smith & Bell, 1985). This procedure gives a fully active, stable enzyme that does not undergo the concentration-dependent polymerization of the unmodified enzyme, which can be used at the high concentrations necessary for the TRNOE experiments described here. NAD was obtained from Boehringer-Mannheim while NADP and 2-oxoglutarate were from Sigma Chemical Co.

Enzyme for use in TRNOE experiments was prepared by sequential dialysis against several changes of 0.1 M potassium phosphate buffer at pH 7 containing 10 μM ethylenediaminetetraacetic acid (EDTA) prepared in 99.8% D_2O and finally against the same buffer prepared with 99.99+% D_2O. Protein concentrations were determined from absorbance at 280 nm (Egan & Dalziel, 1971) with a millimolar extinction coefficient of 52.08 cm^{-1}, using a subunit molecular mass of 56 kDa.

Enzyme used in the binding studies was prepared in similar manner with aqueous buffers.

Ligands used in the TRNOE experiments were subjected to at least four cycles of lyophilization and redissolution in 99.8% D_2O. Small aliquots of concentrated stock solutions were then added to NMR tubes containing enzyme to give the required final concentrations.

Tritiated NAD used in the equilibrium dialysis experiments was obtained from New England Nuclear and was adjusted to the required specific activity with a stock solution of NAD in buffer. All solutions were at pH 7.0.

Equilibrium Dialysis. Aliquots of ligand-free buffer and the stock solution containing the labeled and cold ligand were mixed in screw-top test tubes (total volume 7 mL). One milliliter of the enzyme solution was dialyzed in 10-mm Spectrapore No. 4 dialysis tubing (12000–14000 M_r cutoff). All solutions contained a final concentration of 0.01% (w/v) sodium azide to prevent microbial growth during dialysis, in 0.1 M sodium phosphate buffer and 10 μM EDTA. The pH was 7.0, and dialysis was carried out at room temperature of approximately 22 °C. Protein concentrations were determined as described earlier.

The stoppered test tubes were rotated continuously for 16–18 h. Control experiments showed that equilibrium had been attained and that the protein concentration, within experimental error, did not change during the dialysis.

Binding assays were carried out at least in triplicate. Aliquots of dialyzate or of the equilibrated solution within the dialysis tubing were added to scintillation fluid, and the radioactivity was counted.

Curve Fitting. In general, the binding data were fitted to the Adair equation:

$$[B] = \frac{[P]\sum_{i=1}^{N} iK_i[F]^i}{1 + \sum_{i=1}^{N} K_i[F]^i}$$

where [B] is the concentration of bound ligand, [F] is the concentration of free ligand, and [P] is the total concentration of the unit species to which N classes of ligand binding sites are assumed available. For instance, if two classes of sites are assumed for each subunit in a multimeric protein, then N = 2 and [P] is the subunit concentration. K_i is the ith macroscopic affinity constant.

It was found to be more convenient to fit the data in this manner rather than moving [P] over to the left side of the equation, which then required generation and storage of additional data matrices. The average value calculated for the concentration of the bound ligand was weighted by the reciprocal of the calculated variance of the concentration of the bound ligand. Curve fitting was carried out with the National Institutes of Health Modeling Laboratory curve fitting package. Binding data are displayed in the form of a Scatchard plot of $[B]/e$ versus $[B]/e[F]$, where [B] is the concentration of bound NAD, e is the enzyme concentration, and [F] is the concentration of free NAD in equilibrium with B.

Theoretical Basis of TRNOE. The mathematics, assumptions, and limitations associated with the conformational analysis of bound molecules by the transferred nuclear Overhauser effect (TRNOE) have been rigorously described by Clore and Gronenborn (1983) and Gronenborn and Clore (1985).

From the theory of the steady-state TRNOE, Clore and Gronenborn (1982) showed that in a system where chemical exchange between bound and free states was fast on the chemical shift scale

$$Ni(j) \approx \sigma_{ij}^{BB} \tag{1}$$

and

$$\sigma_{ij}^{BB} \approx (r_{ij}^{BB})^6 \tag{2}$$

where σ_{ij}^{BB} and r_{ij}^{BB} are the cross-relaxation rate and the internuclear distance between the spins i and j, respectively, on the bound state.

Hence, if eq 1 and 2 apply to any two pairs of ligand protons, (i, j) and (i, k), the ratio of the distances from j and k to i in the bound state will be

$$\left[\frac{Ni(k)}{Ni(j)}\right]^{1/6} \approx \left[\frac{\sigma_{ik}^{BB}}{\sigma_{ij}^{BB}}\right]^{1/6} = \frac{r_{ij}^{BB}}{r_{ik}^{BB}} \tag{3}$$

assuming the same correlation time between the two distance vectors r_{ij}^{BB} and r_{ik}^{BB}. Most ligands however contain more than two protons so a multispin system has to be considered. Also, in large proteins (M_r >20K) spin–diffusion is very active (Kalk & Berendsen, 1976). These two considerations cause indirect relaxation between several nuclei to be quite effective, degrading the selectivity of TRNOE measurements. To circumvent these problems, Clore and Gronenborn (1983) developed the theory of time-dependent TRNOE, for the general case of an exchanging system containing multiple spins (as in ligand–protein interactions). They demonstrated from computer simulation and experimental application that the cross-relaxation rates between pairs of bound-ligand protons, or between a bound-ligand proton and protein proton in the ligand–protein complex, can be determined from the initial buildup rates of the time-dependent TRNOEs:

$$\left[\frac{d(NOE)}{dt}\right]_{t=0} = -[(1 - a)\sigma_{ij}^{BB} + a\sigma_{ij}^{FF}] \tag{4}$$

where a is the mole fraction of free ligand and σ_{ij}^{FF} and σ_{ij}^{BB} are the cross-relaxation rates in the free and bound states, respectively, between the spin pairs in subscripts. This enables distance ratios between any two pairs to be obtained, indirect cross-relaxation notwithstanding.

The nonequilibrium condition generating the NOE may include saturation on the free, averaged, or bound resonances (all or singly) or inversion.

Since the ligand may bind to more than one type of site on the protein (e.g., catalytic and regulatory sites on an enzyme), with different cross-relaxation rates (by virtue of different interproton distances or correlation times at each site), eq 4

may be generalized (Gronenborn & Clore, 1985):

$$\left[\frac{d(NOE)}{dt}\right]_{t=0} = -\sum\lambda_I\sigma_{ij}^{BB,I} - \lambda_F\sigma_{ij}^{FF} \quad (5)$$

where λ_I are the mole fractions at sites I (each with its own cross-relaxation rate $\sigma_{ij}^{BB,I}$) and λ_F is the mole fraction of free ligand.

Experimental Methods for TRNOE Measurements. All spectra were obtained on a Bruker WM-360 spectrometer, equipped with a dedicated ASPECT 2000 minicomputer running either the DISNMRP or DISN85 software package. The probe used was a 5-mm Bruker ^1H probe (S:N 100:1 on 0.1% ethylbenzene).

Typically, the tubes used contained glutamate dehydrogenase (GDH) at concentrations of 11.6–19.7 mg/mL, and sample volumes were about 0.35 mL in 5-mm tubes.

In order to minimize dilution, coenzyme and 2-oxoglutarate were prepared as concentrated D_2O solutions containing the same buffers, with the same pH and ionic strength as the enzyme solutions. Addition of between 5 and 15 times excess over the amount calculated to be bound was adequate in achieving desired ligand concentrations in the actual sample. These experiments were conducted at the physiological temperature of 37 °C. Spectra collected under a particular set of conditions were reproducible over several weeks with the same sample, indicating no deleterious time effects on the enzyme at this temperature. Temperatures were measured according to the method of van Geet (Raiford et al., 1979), before and after experimental runs. The probe was tuned and matched only after the sample was equilibrated.

The ^1H spectra of enzyme with ligand were observed with a spectral width of 3597 Hz corresponding to a chemical shift range of 9.98 ppm. Each FID consisted of 8192 data points (4K complex data points). This gave a digitizer resolution of 0.88 Hz/point, which was sufficient to define a ligand peak of typical $V_{1/2}$ of 12 Hz with about 14 points, with 4–5 points present at the apex for peak height measurement. The acquisition time was 1.14 s, and full eight-cycle CYCLOPS phase cycling with quadruple detection was used.

About 800 scans (multiples of 8) were accumulated to give an S:N value of at least 25, and the acquisition pulse used was 13°–20° (0.8–1.2 μs), calculated on the basis of an 11.0-μs, 180° pulse on the residual HDO peak. Special attention was given to the receiver gain to prevent exceeding the digitizer word size. The loss of a few initial points of the FID induced large phase distortions, complicating an already challenging base line.

The pulse sequence and conditions for the TRNOE experiments were very similar to conditions described in Clore and Gronenborn (1983) and will not be detailed further. Particular values are mentioned in the relevant tables themselves.

The worst separation of peaks in the ^1H spectrum (ribose 1's) was 20 Hz, and so the shortest irradiation pulse was of 0.05-s saturation to be effected within the desired selectivity. The power level was found to be 8.8 W (29-dB attenuation of 0.25-W peak output) or 11 mG (based on inversion pulse with decoupler). No warming could be discerned by touch, even with prolonged irradiation at this level.

Water suppression was not done due to the fact that solvent HDO protons constitute effective intermoleculer relaxation partners for spins on the ligand and protein. Indiscriminate spin–diffusion as well as saturation transfer type effects can cause great problems to an NOE spectrum as has been documented in the literature (Gronenborn et al., 1984a,b). Indeed, irradiation on the protein caused a 10% decrease in HDO peak height, presumably by spin-diffusion to a hydration layer bound to protein, but in exchange with bulk solvent.

Time-Dependent TRNOE (td-TRNOE). A relaxation delay of 4 s was used between scans to allow for magnetization recovery prior to perturbation by the selective radio-frequency field. Eight delays ranging from 0.04 ms to 0.6 s were used to obtain plots of intensity change against irradition duration. The initial slopes provide a measure of the cross-relaxation rate directly, and at least four points were employed to define this initial linear region. Preliminary experiments indicated that after about 0.2–0.25 s the curves began to demonstrate curvature. Theoretical expectations (Anderson et al., 1985) of the onset of secondary cross-relaxation are also in agreement. Therefore, six of the eight delays were between 0.04 ms and 0.25 s. Whereas other td-TRNOE studies have included delays up to 0.8 or 1.0 s, the longest value used here was 0.6 s.

Data Processing. The 40 or so files typically obtained per run (eight variable delays, five frequencies) were transferred from the ASPECT 2000 to a MV4000 mainframe computer (Data General).

Spectra were exponentially multiplied by an apodization of −3 Hz (line broadening), Fourier transformed, and phased (using manually preselected values on a representative file), by use of a link option in the NMR1 spectroscopic software package.

Formally, the change in magnetization on irradiation is proportional to the change in intensity. While the area of each peak may in principle be a better approximation, integration was avoided.

First, as it is only the *relative* change of a resonance (with variable durations) which is of interest, the line shape and line width of the peak may be quite rigorously assumed constant and intensity taken as proportional to integrated area. Indeed, it has been the published practice to use the rate of intensity change to reflect the change in the equilibrium magnetizations. Second, an integration procedure relies heavily on the clear definition of a base line. As mentioned, this was not possible. Third, in calculating the area under an absorption mode, Lorentzian line shape, it is necessary to integrate over unreasonably large limits to obtain an accurate measure of the true area encompassed by a Lorentzian line (six line widths for 90% accuracy; 63.6 line width for 99% accuracy; Sotak, 1983).

The intensities were measured by dropping a perpendicular from the apex of the peak to the sketched base line. The process of locating the apex and constructing the perpendicular was assisted by the previously adjusted alignment of peaks in consecutive spectral traces.

The error in the peak intensity measurement was approximated by half the peak to peak noise. This ranged from about 6% for the large peaks at small irradiation times to about 20% for the files with prolonged irradiation (smaller peaks tending toward the full negative TRNOE).

The initial intensity $I(0)$ (at zero irradiation duration) is most important, as it serves as a normalization constant for all subsequent intensities, which are all divided by $I(0)$. The fractions were plotted to give the slopes for the time dependence of TRNOE. Therefore, errors in $I(0)$ affect all slope calculations, with larger values generally giving larger slopes. So, $I(0)$ was determined by plotting the raw intensities obtained from the control irradiation files and extrapolating to zero time. In most cases, the extrapolation was a perfectly horizontal line, as initial control intensities up to 0.2 s were

Chart I

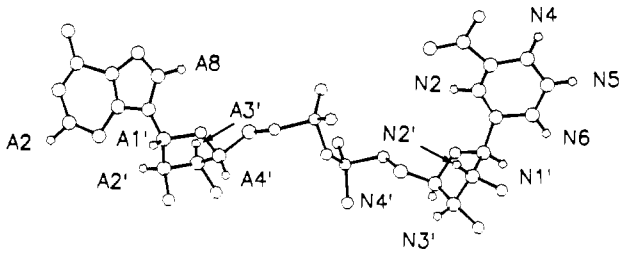

almost all identical (within experimental error), after which there was a gradual decrease due to TRNOEs arising via general spin–diffusion. For those peaks where the extrapolation to zero time was already sloping (negatively), this slope was measured and systematically subtracted from all slopes obtained for these peaks, on irradiating other peaks on interest. In this way, the major effects of rapid spin–diffusion via protein were compensated. The standard errors for the fractions incurred during normalization were calculated as

$$\frac{dz}{z} = \frac{dx}{x} - \frac{dy}{y}$$

and the errors were plotted as bars on the graphs of normalized intensities versus irradiation time and served to guide the estimates of minimum and maximum slopes for each particular plot.

Very recently, Clore and Gronenborn (1985) have extended their simulations to calculate the time dependence of errors involved in interproton distances. The major conclusions drawn by them from this simulation were as follows:

(a) The approximation of eq 3 introduced only minor errors (0.2 Å in the estimate of r_{ik} provided that $\sigma_{SJ} > \sigma_{ij}$ or $\sigma_{ij} > \sigma_{SJ}$).

(b) If the cross-relaxation rate of the S–J vector is greater than that of the reference I–J vector, eq 3 will lead to an overestimation of r_{ik}. If, on the other hand, the cross-relaxation rate of the S–J vector is less than that of the reference I–J vector, the value of r_{SJ} will be underestimated.

Assignment. Peaks were assigned by sequential decoupling of the resonances of pure coenzyme and then by the method of locating "action spectra" (Clore & Gronenborn, 1983). Published spectra of coenzymes bound to other enzymes were also checked.

Results and Discussion

Chemical Shifts. The chemical shifts assigned to the various coenzyme resonances are unaffected by the presence of 2-oxoglutarate. The referencing of spectra to residual HDO appears to be an acceptable procedure since there were only marginal differences in chemical shifts from published literature values [Oppenheimer (1982) referenced to TSP in D_2O solvent]. The numbering of the various protons discussed in this work is shown in Chart I.

The expanded regions upfield and downfield from the residual HDO peaks are shown in Figure 1. Only the downfield set are sufficiently resolved, with clear base line, and were used for intensity measurements. N5 and A2 are almost completely overlapped and, like the ribose 2′ and 3′ peaks, suitable only for irradiation purposes. As shown in Figure 1B, for NAD, N1′ and A1′ are also quite overlaped, and interbase (adenine–nicotinamide) interactions may not be readily inferred from data involving irradiation or observation of these resonances, nor those of the overlapped ribose region. With NADP, the N1′ and A1′ resonances are reversed.

TRNOE's. The data shown in Table I illustrate the effects of irradiation of various ribose protons on either the N2 or the

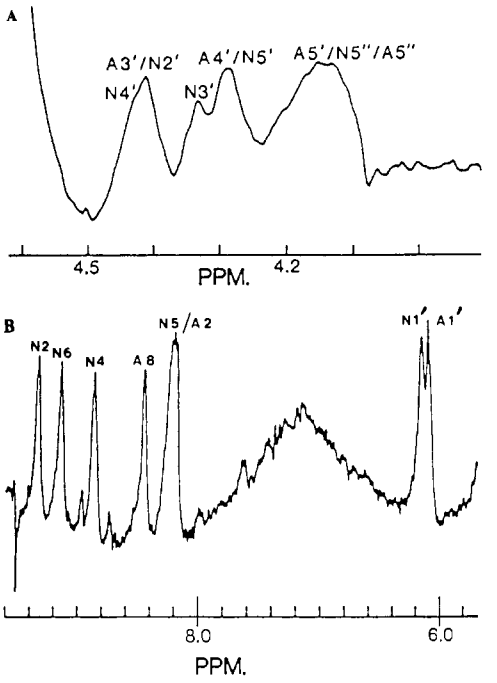

FIGURE 1: (A) 360-MHz ^1H NMR spectrum showing ribose protons upfield from residual HDO. Sample is NAD, 2.47 mM, and GDH, 0.197 mM (in subunits), in phosphate buffer: 256 scans, 4K real points, and 3-Hz line broadening. (B) 360-MHz ^1H NMR spectrum showing the ribose 1′ and base protons of NAD, 2.82 mM, in phosphate buffer with GDH, 0.197 nM: 256 scans, 4K real points, and 3-Hz line broadening.

Table I: TRNOE Measurements on Coenzymes Bound to GDH[a]

irradiated resonance	obsd resonance	NADP	NAD	2-oxoglutarate and NAD
N1′/A1′	N2	0.11	0.07	0.07
N2′/A3′	N2	0.27	0.31	0.24
N3′	N2	0.16	0.15	0.14
N5′,5″	N2	ND	0.13	0.10
N1′	N6	0.20	0.26	0.15
N2′/A3′	N6	0.16	0.10	<ERR
N3′	N6	0.10	0.08	<ERR
N5′/5″	N6	ND	<ERR	<ERR
A1′	A8	0.14	0.15	0.07
A2′	A8	0.30	0.43	0.19
A3′/N2′	A8	0.21	0.22	0.14
A5′,5″	A8	ND	0.20	0.12
N5/A2	N6	0.23	0.27	0.14
N5/A2	N4	0.25	0.33	0.28
N2′/A3′	N1′	0.17	0.16	0.12
A2′	A1′	0.10	0.17	0.12

[a] All TRNOE's are negative. In all cases, the decoupler power was 6 mG and relaxation delay between acquisitions was 1.7 s, while selective irradiation was applied on ligand resonance for 0.44 s. Enzyme concentration was 0.273 mM, NAD concentration was 0.2 mM, and NADP concentration was 3.65 mM. <ERR indicates that the measured TRNOE is less than the experimental error. ND indicates that the TRNOE was not determined.

N6 resonance of the nicotinamide ring.

The data are arranged in sets of rows. The first group of four rows compares the effects of irradiating the nicotinamide ribose protons on the nicotinamide ring proton N2. With NAD, the relatively large TRNOE's observed from N2′ to N2 suggests proximity, which is, of course, possible only with the nicotinamide ring arranged in a syn conformation. The 50–60% smaller values of TRNOE's from N3′ to N2 support this notion, as do the small TRNOE's from N1′ and N2. The significantly larger effect on N2 of irradiation of N1′ (A1′) with NADP raises the possibility of its nicotinamide ring

conformation being a syn–anti mix in the bound state.

The second group of four rows examines the effects of irradiated nicotinamide ribose protons on N6, on the other side of the nicotinamide ring. Here the strong TRNOE effect between N1′ and N6 for NAD signals the existence of predominantly syn conformers. Taken together with the suggestions of the first four rows on N2, an almost exclusively syn conformation of the nicotinamide ring seems virtually certain for NAD^+ both with and without 2–oxoglutarate (columns 2 and 3). $NADP^+$, however, shows significant TRNOE from the ribose N3′ and the overlapped N2′/A3′ peaks to N6, which for proximity now again requires at least a small amount of conformer bound anti. Therefore, two independent features consistently suggest a syn–anti mixture for the nicotinamide ring of $NADP^+$ bound to the enzyme. It appears that $NADP^+$ binds with either a syn conformation or an anti conformation but that free rotation about the glycosidic bond once bound does not occur since this would result in no observable N2′–N6 TRNOE.

The third group of rows shows the effects of ribose irradiation on the adenine A8 proton, and without question, this ring is in an anti conformation. All the enzyme-bound conformations of adenine rings [as NAD(P), cAMP, ADP, or ATP] studied to date by NMR or X-ray methods are anti. Further, the interesting chemistry of coenzyme–dehydrogenase activity concerns hydride transfer with the nicotinamide ring, the adenosine moiety serving essentially as a binding "handle".

The fourth group of four rows constitutes internal calibrations using pairs of protons separated by a fixed distance (N4–N5, N5–N6, all 2.48 Å apart) and by slightly varying distances (2′–1′, 2.5 Å at closest approach, in a ribose 2′-endo conformation, to 2.8 Å in 3′-endo conformation, corresponding to dihedral angles of about 15° and 170°, respectively). The observed inequality of TRNOE between N5–N4 and N5–N6 in columns 2 and 3 is significant. Though several explanations are possible, the real difference in column 3 is probably the presence of the product, 2-oxoglutarate. Indeed, for hydride transfer the 2-carbonyl group must be juxtaposed near the N4 position of the nicotinamide ring *and* between this ring and the N2′, N3′ ribose hydrogen atoms. Of the several such orientations possible (oxo acid moiety over the amide group or over N5, etc.), several of these involve positioning the two methylene groups over and near N5 and N6. Presumably, in these arrangements, the N6 proton would have effective cross-relaxation partners in the nearby methylene protons, in competition with the cross-relaxation effect with N5, thus attenuating the maximum TRNOE possible from irradiating N5.

With NAD in the absence of 2-oxoglutarate we must consider the effects of N3′ and N2′/A3′ irradiation on N6. Although NADP also shows these effects (somewhat larger in magnitude), these can be attributed to the simultaneous presence of syn–anti mixtures as discussed above, and the TRNOE's from N1′ to N2 and N6 confirm this. For NAD however, the TRNOE from N1′ to N2 is very small, considering the generally large TRNOE values observed throughout for this sample. In the purely syn conformation proposed for NAD, N2′ and N6 are about 2.5 Å apart and the N3′–N6 pair approximately between 4 and 5 Å, depending on pucker. Thus, the N2′–N6 and N3′–N6 TRNOE values should be lower than observed. In addition, the N3′–N6 TRNOE should be about 7 times smaller than N2′–N6 TRNOE.

To assist in resolving this anomaly observed with NAD, it is essential to establish the number of NAD molecules bound per subunit in the enzyme. Also, to assist in interpreting the difference discussed here when the coligand 2-oxoglutarate is present, we have examined, by equilibrium dialysis, the binding of [^{14}C]NAD to the enzyme under conditions similar to those used in the NMR experiments.

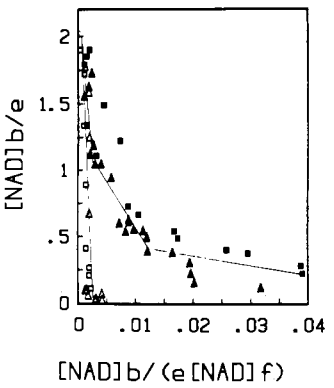

FIGURE 2: Scatchard plots for NAD binding to glutamate dehydrogenase in the absence of coligands (△) and in the presence of 2-oxovalerate (□), glutarate (▲), and 2-oxoglutarate (■).

Equilibrium Binding Data. The equilibrium binding of NAD to the enzyme in the absence of coligand, or in the presence of the monocarboxylic coligand 2-oxovalerate, shown in the form of a Scatchard plot in Figure 2, clearly shows that there exist two NAD sites per monomer, with essentially equal affinity. This raises the possibility of the regulatory site being implicated in generating the anomalous TRNOE effects discussed. These may represent *intermolecular* TRNOE's involving a second coenzyme molecule bound in close proximity to the catalytic site.

In contrast, NAD in the presence of 2-oxoglutarate shows no such effect to N6, indicating an unequivocal, syn conformation. The binding data in the presence of the dicarboxylic acid coligands, glutarate and 2-oxoglutarate (Figure 2), show that although the affinity to one of the two NAD sites per subunit is unaffected, the affinity to the other (presumed to be the active site) is considerably enhanced. As a result, in the TRNOE experiments in the presence of 2-oxoglutarate, only the active site is represented. This indicates that with NAD, in the presence of 2-oxoglutarate, only a syn conformation is present at the active site.

The lack of any evidence for an intermolecular TRNOE in the presence of 2-oxoglutarate (where effectively only the active site contributes) negates the possibility that the active sites are located close to one another at subunit interfaces.

The binding data for NAD in the presence of 2-oxoglutarate (Figure 2) indicate the presence of two sets of three high-affinity sites (the active sites) showing negative homotropic interactions as has been reported previously in the presence of glutarate (Egan & Dalziel, 1972).

Time-Dependent TRNOE's. The time dependence of the TRNOE for selected resonances of the coenzyme was also studied. Figure 3 shows these effects for NAD bound to the enzyme in the absence of coligand. Irradiation selectivity dictated that only certain resonances be investigated in this manner. Three basic sets of conditions were used. First GDH-bound NAD was examined in the absence of coligands. From the binding data shown in Figure 2 it is apparent that in this case the catalytic site and the regulatory site will be equally populated. Next, NADP in the absence of coligands was examined. In this case effective binding is assumed to be only to the active site, with an affinity approximately equal to that of NAD. Finally, enzyme-bound NAD or NADP was examined in the presence of the coligand 2-oxoglutarate. In this case the majority of binding will be at the high-affinity

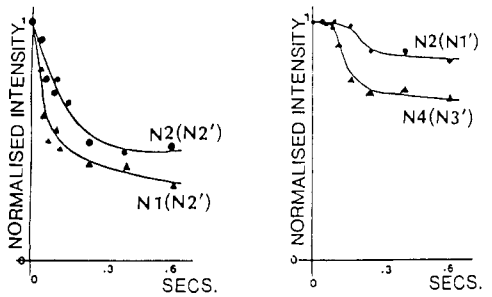

FIGURE 3: Time dependence of the TRNOE for selected resonances of NAD, 2.82 M, with GDH, 0.2 mM (in subunits). Intensities are normalized with respect to intensities obtained on irradiating the control region, 1.75 ppm, for short times. The left panel shows N1 and N2, which are close to N2′, and the slope indicates proximity. The right panel shows examples of lag phases suggesting distance (>5 Å) between N2–N1′ and N4–N3′. The irradiation resonance is in parentheses.

Table II: Time Dependence of TRNOE's and Derived Distances of NAD and NADH Bound to GDH in the Presence of 2-Oxoglutarate[a]

irradiated resonance	obsd resonance	initial slopes, GDH and 2-oxoglutarate		calcd distances (Å)	
		NAD	NADP	NAD	NADP
N1′	N2	lag	lag		
N1′	N6	2.1	1.7	2.5	2.5
N2′	N1′	2.6	2.0	2.3u	2.3u
N2′	N2	2.4	1.9	2.4o	2.4o
N2′	N6	<0.3	lag	>3.5	
N3′	N2	2.1	1.6	2.5	2.5o
N3′	N6	lag	lag		
N3′	N1′	lag			
N5	N6	2.0u		2.5	2.5
N5	N4	2.2u	1.7	2.48*	2.48*
N2′	N6				
N3′	N6				

[a] GDH concentration was 0.2 mM while NAD concentration was 2.82 mM and NADP was 1.43 mM. Decoupler power was 11 mG, and the relaxation delay was 4.0 s. Distances were calculated with eq 3 and 5. (*) Denotes the reference distance. (o) Distance probably overestimated. (u) Distance probably underestimated.

active site, a lesser amount at the low-affinity active site, and an insignificant amount in the case of NAD, at the regulatory site. NADP does not bind effectively to the regulatory site.

The spin pairs listed in Table II are arranged with the irradiated resonance on the left and the observed resonance on the right for experiments with NAD or NADP, both in the presence of 2-oxoglutarate. From the data in Figure 2 it is evident that under these conditions greater than 99% of the bound coenzyme is at the active site.

TRNOE data discussed earlier indicate a single conformation for NAD bound in the presence of 2-oxoglutarate. In addition, the binding data indicate that the majority of the bound NAD under these conditions is contributed by a unique site. With this single-site simplification in hand, and assuming that the single correlation time describing "isotropic" motion of the N5–N6 distance vector is appropriate for describing the motion of all other enzyme-bound distance vectors, we can apply eq 3 to the initial slopes to calculate the actual internuclear distances relative to the N5–N6 distance, which is fixed and taken to be 2.48 Å (Clore & Gronenborn, 1983).

It is apparent from the calculated distances in Table II that the nicotinamide moieties of NAD and NADP adopt remarkably similar conformations at the active site in the presence of 2-oxoglutarate. This is an expected result, considering that these coenzymes have similar dissociation constants from this site and, moreover, are structurally identical,

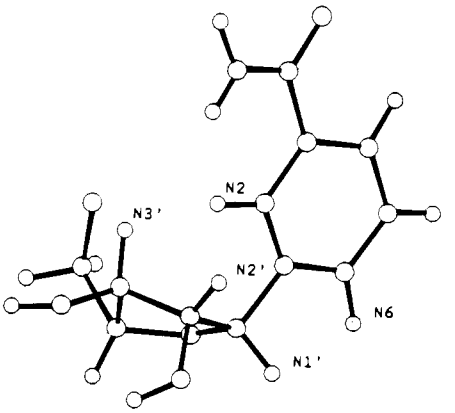

FIGURE 4: Overall best fit conformation of coenzyme bound to glutamate dehydrogenase. The approximate conformation of the nicotinamide end of the coenzyme, bound in the presence of 2-oxoglutarate. The TRNOE-derived distances between labeled protons (Table II) are consistent with a conformation in which the nicotinamide ring is syn and the ribose pucker is in the C(3′)-endo range.

Table III: Time Dependence of TRNOE and Derived Distances for NAD Bound to GDH as Binary Complex[a]

irradiated resonance	obsd resonance	initial slope	calcd distances at regulatory site (from eq 6) (Å)
N1′	N2	lag	
N1′	N6	1.7	2.3
N2′	N1′	1.7	2.3
N2′	N2	2.2	
N2′	N6	1.1	2.3
N3′	N2	1.7	2.9
N3′	N1′	1.6	2.2[b]
N3′	N6′	1.3	2.2[b]
N5	N4	1.4	2.48[c]

[a] GDH concentration was 1.2 mM while NAD concentration was 2.82 nM. Decoupler power was 1 mG, and the relaxation was 5.0 s. [b] Intermolecular distances—see text. [c] Denotes reference distance.

except for the extra 2′-phosphate on the adenosine ribose in NADP.

On the basis of the proton–proton distances derived from time-dependent TRNOE's (Table II), the approximate conformation of the nicotinamide end of the cofactor can be modeled. The starting point for this model was the high-resolution X-ray structure of free NAD^+ (Parthasarathy & Fridey, 1984). All C–H bond lengths were normalized to 1.05 Å. The nicotinamide ring was then rotated about the glycosyl bond in order to achieve the best fit between NOE-derived and model-derived interproton distances. The nicotinamide ribose was allowed various puckers in the C(2′)- and C(3′)-endo ranges (Altona & Sundaralingam, 1972). These conformations are observed in almost all NAD structures (Parthasarathy & Fridey, 1984; Grau, 1982) and are the preferred puckering modes for nucleosides in general (Saenger, 1984).

Modeling results indicate that the observed interproton distances for N2–N2′ and N6–N1′ (Table II) can only be achieved if the nicotinamide glycosidic torsion angle is syn or high syn (approximately 70°–110°). Further, observation of an N2–N3′ TRNOE suggests that the puckering of the nicotinamide ribose falls within the C(3′)-endo range of the pseudorotation cycle (Altona & Sundaralingam, 1972). A C(3′)-endo pucker places both the N3′ proton and the nicotinamide ring in an axial orientation relative to the ribose ring. In this conformation, the N3′ proton can achieve the observed 2.48-Å distance from N2. The C(3′)-endo pucker also places N2′ and N1′ equitorial, minimizing the distance between these protons as well (Figure 4).

We now turn to the more complex case of NAD alone with GDH shown in Table III. Equilibrium binding studies indicate the presence of two weak sites per subunit (K_d approximately 0.75 mM). Consequently, the estimated mole fractions of 0.064 at each site are highly approximate.

An approximate conformation of NAD bound to the regulatory site in the absence of 2-oxoglutarate can be obtained, making certain assumptions. First, we assume that the correlation time for the N5–N6 vector is the same at both catalytic and regulatory sites (isotropic motion). Thic correlation time ($J_{5'6}$) can then be calculated by applying eq 5 given the assumption that rapid exchange exists between the free and bound sites; hence, J is approximately 0 (Clore & Gronenborn, 1983).

Since λ_{cat} is approximately $\approx\lambda_{reg}$, eq 3 can be substituted into eq 5 and rearranged to give

$$\frac{1}{(r_{ij})^6_{reg}} = \left(\left.\frac{d(NOE)}{dt}\right|_{t=0} \times \frac{1}{\lambda_{cat}(J_{5-6})(r_{5-6})^6} \right) - \frac{1}{(r_{ij})^6_{cat}} \quad (6)$$

where reg and cat denote regulatory and catalytic sites, respectively.

A semiqualitative estimate can be made of internuclear distances at the regulatory site (r_{ij}, reg) from eq 6 given that the conformation of NAD at the catalytic site in the absence of 2-oxoglutarate (r_{ij}, cat) is the same as that obtained for NAD(P) with 2-oxoglutarate present Table II).

The presence of a lag in the td-TRNOE between N1′ and N2 (Table III) suggests that N2 is *not* nearby in an anti conformation, at *either* regulatory or catalytic sites. However, significant TRNOE's from N2′ and N3′ to N6 imply short distances in the regulatory site (catalytic site already assumed syn, and hence not contributing to N2′–N6 or N3′–N6). Yet, N6 is close to N2′ and N3′ only in an anti conformation, when N1′–N2 are also quite close. This apparent contradication could be caused by an intermoleculer, ribose N2′ N3′ and base N6 cross-relaxation. Indeed, in a syn comformation, N6 is at the molecular periphery and may be positioned close to the nicotinamide ribose of another coenzyme molecule. This would explain the paradox of the short distances calculated, which are not realizable in any syn comformation. N1′, at the periphery too, is noticed to be closer to N2′ (2.27 Å) than physically possible (2.5 Å) and may also be demonstrating the intermolecular effect. This intermolecular effect is further confirmed by the existence of an N3′–N1′ effect (Table III) for NAD in the absence of 2-oxoglutarate. As with the N3′–N6 pair, N3′–N1′ gives a lag in the presence of 2-oxoglutarate indicating the lack of an intramolecular effect. Hence, the distances calculated from the initial slopes in Table III for these two pairs are intermolecular distances.

Table III assumes only two sites, the active site and the regulatory site, and on this basis the rough distances obtained for the regulatory site (barring N2′, or N3′, to N6) are indicative of a syn conformation not unlike that in the catalytic site itself. If the nicotinamide moieties at both sites are syn (as indicated by the N1′–N2 lag), then the N2′ or N3′ to N6 and N3′ to N1′ effects must arise from a situation where nicotinamide moieties are neighboring. These tentative intermolecular distances, N2′–N6 (2.3 Å), N3′–N6 (2.2 Å), and N3′–N1′ (2.2 Å), should be recognized as being very rough, but certainly less than 5 Å (or a non-zero slope would not be seen).

The observation of a possible N2′, or N3′, to N6 interaction is not evident in the ternary complexes of NAD(P) (with 2-oxoglutarate and GDH), which are where the TRNOE's are essentially dominated by coenzyme occupancy at the catalytic sites, and hence, the possibility of adjacent catalytic sites may be eliminated.

In both the TRNOE experiments and the time-dependent TRNOE study reported here, we obtain evidence that the coenzyme nicotinamide moieties of NAD bound to the active and regulatory sites on a subunit of glutamate dehydrogenase are located in close proximity to each other. The idea that the active and regulatory coenzyme binding sites of glutamate dehydrogenase are located near one another was first postulated on the basis of binding studies (Cross & Fisher, 1970). The present work is the first direct indication that this may be so. Because a number of two-site models consistent with the measured proton–proton distances can be constructed, we do not discuss in detail any one model for coenzyme–coenzyme interaction.

For NADP binding to GDH in the absence of 2-oxoglutarate, the td-TRNOE results are in agreement with the TRNOE results discussed earlier. Thus, in marked contrast to the ternary complexes of NAD(P) (with GDH and 2-oxoglutarate) and the binary complex of NAD, in the binary complex with NADP, NADP is probably bound with roughly equal amounts of syn and anti conformations present at the catalytic site. The 2′-phosphate on the adenosine ribose of NADP must, therefore, play a role in preventing complete syn binding, while the presence of 2-oxoglutarate restores the selectivity required to achieve the complete stereo preference of hydride transfer.

ACKNOWLEDGMENTS

We thank R. Parthasarathy for making available the coordinates of NAD.

REFERENCES

Alex, S., & Bell, J. E. (1980) *Biochem. J. 191*, 299–304.
Altona, C., & Sundaralingam, M. (1972) *J. Am. Chem. Soc. 94*, 8205–8212.
Anderson, N. H., Nguyen, K. T., & Eaton, J. L. (1985) *J. Magn. Reson. 63*, 365–382.
Appella, E., & Tomkins, G. M. (1966) *J. Mol. Biol. 18*, 77–89.
Bailey, P. M., & O'Neill, K. T. J. (1980) *Eur. J. Biochem. 112*, 521–531.
Bell, E. T., LiMuti, C., Renz, C. L., & Bell, J. E. (1985) *Biochem. J. 225*, 209–217.
Bell, J. E., & Dalziel, K. (1973) *Biochim. Biophys. Acta 3*, 237–242.
Birkhoft, J. J., Miake, F., Banazsak, L. J., & Frieden, C. (1979) *J. Biol. Chem. 254*, 4915–4918.
Bothner-By, A. A., & Gassend, R. (1973) *Ann. N.Y. Acad. Sci. 222*, 668–676.
Clore, G. M., & Gronenborn, A. M. (1983) *J. Magn. Reson. 53*, 423–442.
Clore, G. M., & Gronenborn, A. M. (1985) *J. Magn. Reson. 61*, 158–164.
Cross, D. G., & Fisher, H. F. (1970) *J. Biol. Chem. 245*, 2612–2621.
Dalziel, K., & Egan, R. R. (1972) *Biochem. J. 126*, 975–984.
Egan, R. R., & Dalziel, K. (1971) *Biochim. Biophys. Acta 250*, 47–50.
Engel, P. C., & Dalziel, K. (1969) *Biochem. J. 115*, 621–631.
George, A., & Bell, J. E. (1980) *Biochemistry 19*, 6057–6061.
Grau, U. (1982) *The Pyridine Nucleotide Coenzymes* (Everse, J., Anderson, B., & You, K.-S., Eds.) pp 135–187, Academic, New York.
Gronenborn, A. M., & Clore, G. M. (1984) *Prog. Nucl. Magn. Reson. Spectrosc. 17*, 1–62.

Gronenborn, A. M., Clore, G. M., & Jeffrey, J. (1984a) *J. Mol. Biol. 172*, 559–572.
Gronenborn, A. M., Clore, G. M., Hobbs, L., & Jeffrey, J. (1984b) *Eur. J. Biochem. 145*, 365–371.
Harris, R. K. (1983) *Nuclear Magnetic Resonance Spectroscopy*, Pitman, London.
Jallon, J.-M., & Iwatsubo, B. (1971) *Biochem. Biophys. Res. Commun. 45*, 964–971.
Kalk, A., & Berendsen, H. C. J. (1976) *J. Magn. Reson. 24*, 343–366.
Levy, H. R., & Vennesland, B. (1957) *J. Biol. Chem. 228*, 85–92.
Levy, H. R., Ejchart, A., & Levy, G. C. (1983) *Biochemistry 22*, 2792–2796.
LiMuti, C., & Bell, J. E. (1983) *Biochem. J. 211*, 99–107.
Mire, M., & Cohen, R. (1971) *Eur. J. Biochem. 23*, 276–281.
Oppenheimer, N. J. (1982) *The Pyridine Nucleotide Coenzymes* (Everse, J., Anderson, B., & You, K.-S., Eds.) Chapter 3, Academic, New York.
Parthasarathy, R., & Fridey, S. M. (1984) *Science (Washington, D.C.) 226*, 969–971.
Raiford, D. S., Fisk, C. L., & Becker, E. D. (1979) *Anal. Chem. 51*, 2050–2051.
Saenger, W. (1984) *Principles of Nucleic Acid Structure*, pp 55–65, Springer-Verlag, New York.
Smith, E. L., Austen, B. M., Blumenthal, K. M., & Nye, J. F. (1975) *Enzymes (3rd Ed.) 11*.
Smith, T. (1985) Ph.D. Dissertation, University of Rochester.
Smith, T., & Bell, J. E. (1982) *Biochemistry 21*, 733–737.
Smith, T., & Bell, J. E. (1985) *Arch. Biochem. Biophys. 239*, 63–73.
Sotak, C. H. (1983) Ph.D. Dissertation, Syracuse University.
You, K. (1982) *Methods Enzymol. 87*, 101–125.
You, K., Arnold, L. J., Allison, W. S., & Kaplan, N. O. (1978) *Trends Biochem. Sci. (Pers. Ed.) 3*, 265–268.

Adenosine Deaminase Converts Purine Riboside into an Analogue of a Reactive Intermediate: A ^{13}C NMR and Kinetic Study†

Linda C. Kurz* and Carl Frieden

Department of Biological Chemistry, Division of Biology and Biomedical Sciences, Washington University School of Medicine, St. Louis, Missouri 63110

Received March 4, 1987; Revised Manuscript Received August 18, 1987

ABSTRACT: The ^{13}C NMR spectra of [2-^{13}C]- and [6-^{13}C]purine ribosides have been obtained free in solution and bound to the active site of adenosine deaminase. The positions of the resonances of the bound ligand are shifted relative to those of the free ligand as follows: C-2, −3.7 ppm; C-6, −73.1 ppm. The binary complexes are in slow exchange with free purine riboside on the NMR time scale, and the dissociation rate constant is estimated to be 13.5 s^{-1} from the slow exchange broadening of the free signal. In aqueous solution, protonation of purine riboside at N-1 results in changes in ^{13}C chemical shift relative to those of the free base as follows: C-2, −4.9 ppm; C-6, −7.9 ppm. The changes in chemical shift that occur when purine riboside binds to the enzyme indicate that the hybridization of C-6 changes from sp^2 to sp^3 in the binary complex with formation of a new bond to oxygen or sulfur. A change in C-2 hybridization can be eliminated as can protonation at N-1 as the sole cause of the chemical shift changes. The kinetic constants for the adenosine deaminase catalyzed hydrolysis of 6-chloro- and 6-fluoropurine riboside have been compared, and the reactivity order implies that carbon–halogen bond breaking does not occur in the rate-determining step. These observations support a mechanism for the enzyme in which formation of a tetrahedral intermediate is the most difficult chemical step. Enzymic stabilization of this intermediate may be an important catalytic strategy used by the enzyme to lower the standard free energy of the preceding transition state.

Adenosine deaminase (EC 3.5.4.4) catalyzes the hydrolysis of (deoxy)adenosine to (deoxy)inosine. Purine riboside, which lacks a leaving group at C-6, is an unreactive adenosine analogue and a potent reversible inhibitor of the enzyme (Wolfenden et al., 1969).

The structures of both the ligand and the enzyme are perturbed when purine riboside binds to adenosine deaminase (Kurz & Frieden, 1983; Kurz et al., 1985). The binding is accompanied by a large UV difference spectrum, and the solvent isotope effect on the binding constant, $K_i(H_2O)/K_i(D_2O) = 1.5$, is quite substantial. Studies of acrylamide quenching of protein fluorescence indicate decreased solvent accessibility of protein tryptophan residues in enzyme–inhibitor complexes (Kurz et al., 1985).

In order to account for the UV difference spectra and solvent isotope effect data, we previously proposed three possible structures for the complexed purine riboside (Kurz & Frieden, 1983): protonation at N-1, covalent adduct formation (possibly with a sulfhydryl residue) at C-2, or covalent adduct formation at C-6 (Figure 1). We now present evidence from ^{13}C NMR which supports covalent adduct formation or hydration at C-6.

This observation together with new data on the relative reactivity of 6-F- and 6-Cl-substituted purine ribosides supports a mechanism for the enzyme in which formation of a tetra-

†Supported by National Institutes of Health Grant GM33851 to L.C.K. and National Institutes of Health Grant DK13332 to C.F. The Washington University High Resolution NMR Service Facility is funded in part through NIH Biomedical Research Support Shared Instrument Grant 1 S10 RR02004 and a gift from the Monsanto Co.

0006-2960/87/0426-8450$01.50/0